PROCEEDINGS OF THE REMOTE SENSING AND PHOTOGRAMMETRY SOCIETY
CONFERENCE Remote Sensing and the Carbon Cycle, Burlington House, London, 5th May 2010.

# Integration of PS-InSAR and GPS for monitoring seasonal and long-term peatland surface fluctuations

Zhou, Z., Waldron, S., Li, Z.

*Department of Geographical and Earth Sciences*
*University of Glasgow, Glasgow G12 8QQ*
*Email: Zhiwei.Zhou@ges.gla.ac.uk*

## Abstract

*Due to water table elevation changes and entrapped gas ebullition, vertical fluctuations in peatlands surface of up to 20 cm have been reported. Combined with GPS measurement, persistent scatterers synthetic aperture radar interferometry (PS-InSAR) has acquired huge success in diverse areas in recent years. In this paper, we explain our approach to assessing the viability of PS-InSAR technology to map seasonal and long-term peatland surface oscillation. Loss of coherence is proving challenging, and we discuss this and our approach to assessing how to overcome coherence loss.*

**Keywords:** *PS-InSAR, GPS, coherence, peatland surface fluctuations*

## 1. Introduction

Due to their capacity to store carbon, peatlands are an important reservoir in the global carbon cycle, and may also serve as a source or sink for atmospheric carbon dioxide ($CO_2$) (Charman. *et al.*, 2008). Studies related to greenhouse gas (GHG) emissions from peatlands and their response to climate changes have increased during recent years with recent interest including assessments of surface level fluctuations in relation to GHG fluxes. For example, a consistent relationship was reported between the periods of increased and decreased free phase gas content and surface deformation by using ground penetrating radar, combined with elevation rod and gas flux measurements (Comas *et al.*, 2008).

In recent decades, Interferometric Synthetic Aperture Radar (InSAR) has been employed to measure the Earth's surface movements with sub-centimetre precision and tens of metres horizontal spatial resolution over large regions (e.g. 100 km × 100 km). This has led to many new insights into geophysical and engineering processes, e.g., volcanoes (Massonnet and Feigl, 1998), and observations of seasonal ground deformation with the advent of Persistent Scatterers InSAR techniques (Colesanti et al., 2003).

Our research is investigating whether PS-InSAR/GPS integrated techniques can be used to map spatiotemporal deformation of peatlands, and link this to their biogeochemical functioning. In our broader study, we will try to investigate:

1) Seasonal peatland surface fluctuation;
2) Long term peatland surface deformation velocity in the satellite Line Of Sight (LOS);
3) The relationship between fluctuation magnitude and environmental factors including water level, atmospheric pressure, and temperature.

Should this approach be successful it will enable monitoring of peatland landscapes largely inaccessible to field approaches, and fluctuations over a much wider scale manageable in field approaches. Here we outline our progress to date in assessing the viability of this technique to study peatland surface variation.

## 2. PS-InSAR

Radar Interferometry exploits two radar images acquired at different time, generates interferograms after sub-pixel registration and reveals the surface changes by calculating the phase contained in the interferogram (Richard and Philipp, 1998, Massonnet and Feigl, 1998). Atmospheric fluctuation (particularly the part due to atmospheric water vapour) is the main error source in applying conventional InSAR, and can be corrected using independent atmospheric water vapour products such as GPS, National Aeronautics and Space Administration (NASA) Moderate Resolution Imaging Spectroradiometer (MODIS) or European Space Agency (ESA) Medium Resolution Imaging Spectrometer (MERIS) (Li et al., 2009). However, conventional InSAR will fail to detect surface deformation signals in a highly-vegetated site (e.g. peatlands) due to temporal decorrelation caused by vegetation. Persistent Scatterers Interferometry (PS InSAR) allows moderation of the atmospheric disturbance and other sources of errors (e.g. orbital and DEM errors) by identification and exploitation of natural reflectors that provide good coherence and stable phases in a long temporal series of interferograms (Ferretti et al., 2001). Starting from the characters of phase, a new persistent scatters selection algorithm (i.e. Stanford Method for Persistent Scatterers, StaMPS) that can be applied to non-urban areas has been developed (Hooper et al., 2004, Hooper et al., 2007), and it is this method that is applied in this study.

## 3. Study area and methods

The peatland study area, Flanders Moss (Fig. 1), is one of the largest sites of a lowland raised bog in Britain and one of the most intact raised bogs in Europe. Flanders Moss is located at (56.1665°N, 4.2014°W). Bounded by the River Forth, Flanders Moss is roughly circular with four low domes and separated by shallow valleys. Many of the classical raised bog features can be observed in Flanders Moss. *Sphagnum* and *eriophorum* comprise the dominant vegetation with lesser amounts of *calluna* and wood. The depth of peat ranges from 1.80m to 6.87m (Ewan Group plc, 2006).

The study has been carried out using two tracks of Envisat ASAR images: seven acquisitions from track 15 (ascending) and seven from track 223 (descending). The data has been analysed using the StaMPS package developed at Stanford University, USA (Hooper et al., 2007). Topographic contributions were removed using a 90 m Shuttle Radar Topography Mission (SRTM) digital elevation model (Farr et al., 2007).

## 4. Results

Figure 1 shows all the PS points detected over the study area: about 77 PS points for the ascending track (indicated by yellow points), and about 96 PS points for the descending (indicated by blue points). The locations of most PS points from the two tracks are different, which could be due to (1) the different satellite geometries of these two tracks, and/or (2) the uncertainties in interferogram geocoding.

Three small areas (i.e. A, B and C in Figure 1) were chosen to investigate the surface movement evolution during the period between April 2003 and July 2006, shown in Figures 2(a), 2(b) and 2(c) respectively. It is clear that: (1) all the PS points exhibit negative LOS range changes (i.e. moving away from satellite); (2) for a specific track, the deformation time series of all the PS points in a small area are consistent with each other; and (3) for each area, the magnitudes of the total LOS range changes from ascending track are greater than those from descending track.

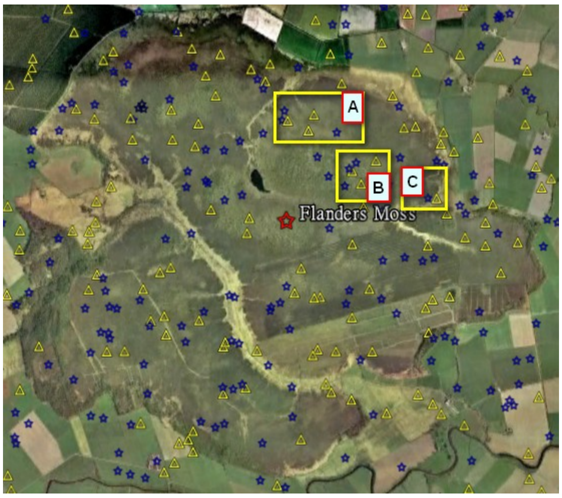

Figure 1: Flander Moss (Source: Google Earth)

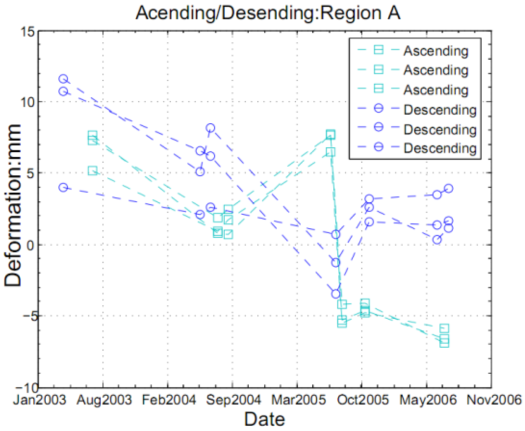

Figure 2a: LOS range change time series in region A

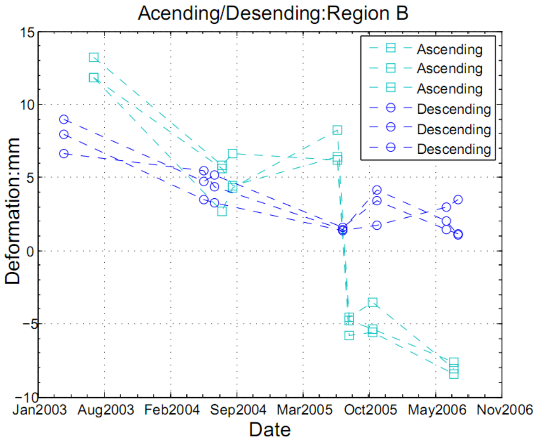

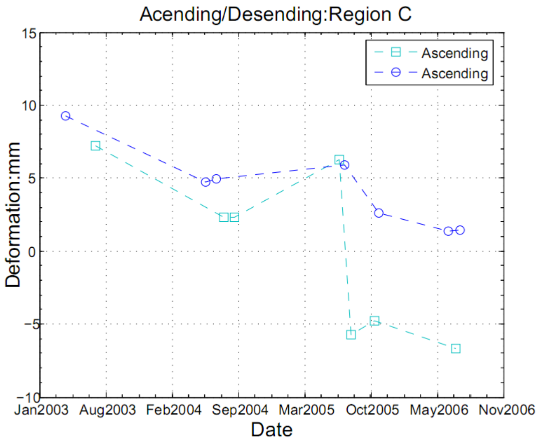

Figure 2b LOS range change time series in region B   2c LOS range change time series in region C

Note: light blue points represent LOS range change time series of PS points from ascending track 015 whilst blue points indicate those from descending track 223.

## 5. Discussion and conclusion

The surface level fluctuation recorded in peatlands by others are of sufficient magnitude to be detected by InSAR technology. This preliminary investigation of radar interfeometry to detect peatland surface fluctuations has yielded some encouraging results showing change in vertical surface of comparable magnitudes, but there are many more challenges ahead. There two possibilities to improve the coherence in peatlands: (1) to use long wavelength SAR images such as L-band JERS and ALOS datasets, and (2) to install comer reflectors over the study area. Next we are going to employ L-band SAR images to further investigate the surface movements in Flander Moss, and GPS measurements may also be collected for validation purposes.

**Acknowledgements:** Zhiwei Zhou is funded by the Chinese Scholarship Council Scheme and the University of Glasgow.

## References

CHARMAN., D. J., JOOSTEN., H., LAINE., J., LEE., D., MINAYEVA., T., OPDAM., S., PARISH., F., SILVIUS., M. & SIRIN., A. 2008. *Assessment on Peatlands, Biodiversity and Climate Change: Main Report,* Wageningen, Global Enviroment Centre, Kuala Lumpur & Wetlands International.

COLESANTI, C., FERRETTI, A., NOVALI, F., PRATI, C. & ROCCA, F. 2003. SAR monitoring of progressive and seasonal ground deformation using the permanent scatterers technique. *Geoscience and Remote Sensing, IEEE Transactions on,* 41**,** 1685-1701.

COMAS, X., SLATER, L. & REEVE, A. 2008. Seasonal geophysical monitoring of biogenic gases in a northern peatland: Implications for temporal and spatial variability in free phase gas production rates. *J. Geophys. Res.,* 113**,** G01012.

EWAN GROUP, P. 2006. Flanders Moss National Nature Reserve:review of hydrological monitor strategy. Scottish Natural Heritage Commissioned Report No. 168 (ROAME No. FO3LG05).

FARR, T. G., ROSEN, P. A., CARO, E., CRIPPEN, R., DUREN, R., HENSLEY, S., KOBRICK, M., PALLER, M., RODRIGUEZ, E., ROTH, L., SEAL, D., SHAFFER, S., SHIMADA, J., UMLAND, J., WERNER, M., OSKIN, M., BURBANK, D. & ALSDORF, D. 2007. The Shuttle Radar Topography Mission. *Rev. Geophys.,* 45**,** RG2004.

FERRETTI, A., PRATI, C. & ROCCA, F. 2001. Permanent scatterers in SAR interferometry. *Geoscience and Remote Sensing, IEEE Transactions on,* 39**,** 8-20.

HOOPER, A., SEGALL, P. & ZEBKER, H. 2007. Persistent scatterer interferometric synthetic aperture radar for crustal deformation analysis, with application to Volcán Alcedo, Galápagos. *J. Geophys. Res.,* 112**,** B07407.

HOOPER, A., ZEBKER, H., SEGALL, P. & KAMPES, B. 2004. A new method for measuring deformation on volcanoes and other natural terrains using InSAR persistent scatterers. *Geophys. Res. Lett.,* 31**,** L23611.

LI, Z., FIELDING, E. J. & CROSS, P. 2009. Integration of InSAR Time-Series Analysis and Water-Vapor Correction for Mapping Postseismic Motion After the 2003 Bam (Iran) Earthquake. *Geoscience and Remote Sensing, IEEE Transactions on,* 47**,** 3220-3230.

MASSONNET, D. & FEIGL, K. L. 1998. Radar Interferometry and Its Application to Changes in the Earth's Surface. *Rev. Geophys.,* 36**,** 441-500.

RICHARD, B. & PHILIPP, H. 1998. Synthetic aperture radar interferometry. *Inverse Problems,* 14**,** R1-R54.